Journal of Engineering Sciences
Vol 11, Issue 5,May/ 2020
ISSN NO: 0377-9254

THEORETICAL CONDUCTIVITY AND ELECTRON DENSITY ANALYSIS OF AU AND S SUBSTITUTED 1,4-BIS(2-CYCLOPENTYLETHYL)CYCLOHEXANE AND 1,4-BIS(2-(TETRAHYDROTHIOPHEN-2-YL)ETHYL)CYCLOHEXANE NANOWIRE

Jayalakshmi P[1], Selvaraju K. [*1] and Nidhin P V [2],

[1]*Department of Physics, Kandaswami Kandar's College, Velur, 638182, India*

[2]*Department of Physics, Safa college of Arts and Science , Valanchery, Kerala, India*

Abstract

The examination of sub-atomicnanowires1,4-bis(2-cyclopentylethyl)cyclohexane and 1,4-bis(2-(tetrahydrothiophen-2-yl)ethyl)cyclohexane) incorporating the spatial distribution of electron within the system, was completed utilizing elevated level Density Functional Theory (DFT) with the assistance of LANL2DZ premise set combined with the Bader's hypothesis. All the investigations were completed within the sight of an applied electric field which is step by step expanding from 0.05–0.26VÅ−1. The impact of the applied electric field on the geometrical and the topological examination of the atomic wire is completely made and contemplates were made to characterize the properties of the nanowires based on the polarity and conducting nature. HOMO-LUMO examination were made to decide the manner in which the one dimensional nanowires initiates conduction. The IV characteristics and the ESP surface were generated for the nanowires to exemplify the nature of the conducting nanowires.

***Keywords*— charge density analysis, Nanowires, DFT optimizations, I-V characteristics.**

1. INTRODUCTION

Nanowires can be characterized as structures that have a sidelong size compelled to several nanometers or less and an unconstrained longitudinal size. Three-dimensional nanostructures have been concentrated seriously basically because of the properties emerging from an exchange of low dimensionality and quantum impacts in the development of nanoscale gadgets **[1].** One dimensional metal nano structures are an importand area of research due to their optical, electronic, magnetic and thermal properties **[2].** The current research consolidates the effect of varying electric filed over gold and Sulphur substituted one dimensional nanowire. The variations in the topological parameters combined with the conducting nature were analyzed in the current research. The variation of the electrostatic potential field of the isolated molecule with the increasing electric field was analyzed in detail to reveal the expected stability while generating the molecular wire. Fig.1 shows the geometrically optimized 1,4-bis(2-cyclopentylethyl)cyclohexane [hereafter abbreviated as biscyclo (W1)] and 1,4-bis(2-(tetrahydrothiophen-2-yl)ethyl)cyclohexane [hereafter abbreviated as bisthio (W2)] nano wires.

2. COMPUTATIONAL DETAILS

The W1andW2 nano wires, with five field measures within the range of ±0.26 V/Å are minimized for zero and higher applied electrical fields using the DFT method integrated in the Gaussian03 software package [3]. The DFT calculations were carried out by incorporating the Beckes three parameters exchange function and Lee, Yang and Parr gradient-corrected correlation factor (B3LYP) **[4]** along with double zeta basis set as it provides complete explanation of heavy metal atoms in the molecular wire. The structural energy minimization was tested by means of the Berny algorithm and the optimization converges with the threshold value of 0.00045, 0.0003, 0.0018 and 0.0012 au for maximum force, root mean square force (RMS),

maximum displacement and RMS displacement respectively. The current research analyzed the effect of varying electric field over the geometry as well as the topological parameters associated with the nano wires. From the quantum theory of atoms in molecules (QTAIM), the bond topological and electrostatic properties were predicted via the EXT94b module implemented in the AIMPAC software[5].DENPROP and wfn2plots were used to create two dimensional grids to map deformation and Laplacian contour plots. The conducting nature of the nano wire was justified by determining the I-V characteristics of the wire with the varying electric field. The gaussian visualizing package GVIEW-5 was used to explore the three-dimensional surface plots. The density of states (DOS) for different applied EFs was well framed from the Gauss Sum program.[6].

3. RESULTS AND DISCUSSION

3.1. STRUCTURAL ASPECTS

The superimpose plot of optimized structures of W1 and W2 molecular nano wire was depicted in the fig. 2. In both the wires gold atom (as an electrode) was attached at both the ends through Sulphur atom. The two cyclopentane rings on either side of the six membered rings in W1 nanowire was replaced with two thiophene rings in W2 molecular nano wire. As the geometry variation is correlated with the molecular conductivity, it is highly essential to investigate the structural change of W1 and W2 molecular nano wire over the wide range (0 to 0.26V/Å) of applied electric field. The C-C bond lengths of six membered rings in both the molecule ranges from 1.390 to 1.461 Å [W1] and 1.392 to 1.462 Å [W2] with the maximum variation of 0.01 Å when the applied electric field is increased from 0 V/Å. Similarly, the average C-C bond lengths of Cyclopentane and thiophene rings of W1 and W2 is 1.453 Å and 1.508 Å for the 0V/ Å, and the same was increased feebly by 0.001 Å, when the electric field is increased to 0.26 V/ Å. As seen in the Fig. 2, it was observed that maximum variation was noticed in terminal bonds (Au-S and S-C) of both the system, when it was subjected with different level of applied electric field. The applied electric field made a significant effect over the S-C terminal bonds in both the left and right end of both the molecular nanowires. The maximum deviation of about 0.01 Å [left] and 0.03 Å [right] is found when the increasing electric field from zero bias condition. Similar variation was also observed for Au-S bond lengths with the maximum difference of 0.03 Å [left] and 0.09 Å [right] when the field increased from 0 to 0.26 V/Å.

3.2. CHARGE DENSITY AND LAPLACIAN OF ELECTRON DENSITY

The Quantum hypothesis of Atoms in Molecule hypothesis built up by Bader was prescribed to explore the distribution of electrons and the density along with the electrostatic properties of confined isolated molecule **[7]**. The two-dimensional contour plots of disfigurement of electron density maps of the concerned nanowire for the applied electric fields are appeared in the Fig. (4). The studies exposed that the electron density of C-C bonds of W1 and W2 nano wire were affected by the external varying electric field. Ultimate charge density of 2.054 $eÅ^{-3}$ is examined for C(7)-C(8)/ C(16)-C(9) bonds which reduced to ~2.01 $eÅ^{-3}$ when EF gradually increased to 0.26 V for W1 wire. The density was found to be decreasing with the increasing electric field. A dominant decrease was observed in C(1)-C(6) for W1 from 1.882 $eÅ^{-3}$ to 1.885 $eÅ^{-3}$, whereas the density was found increasing to limit of ~0.03 for various C-C bonds of the same molecule. Considerable increase from 1.754 $eÅ^{-3}$ to 1.807 $eÅ^{-3}$ for C(9)-C(3) chemical bond, justifying the fact that the effect of the varying electric field depends on the position of the chemical bonds. Comparatively lesser electron density is detected in the terminal bonds between Au-S, ranging from 0.4 to 0.5 $eÅ^{-3}$, The result exposed that the charge density increased from 0.494 $eÅ^{-3}$ to 0.522 $eÅ^{-3}$ in Au(15)-S(14) whereas contradictory result observed for S(21)-Au(22) spotting the decrease from 0.494 $eÅ^{-3}$ to 0.421 $eÅ^{-3}$. Similar outcome is observed in the case of W2 nano wire subjected to the varying field. A maximum charge density of 2.066 $eÅ^{-3}$ is noticed in the C(17)-C(9) / C(7)-C(8) bonds which reduced to 2.028 $eÅ^{-3}$ /2.04 $eÅ^{-3}$ when electric field is increased from 0 to 0.26 V. The effect of the field on the terminal bonds S(15)-Au(16) / Au(24)-S(23) were similar to W1 wire, where the density increased from 0.501 $eÅ^{-3}$ to 0.516 $eÅ^{-3}$ and reduced from 0.497 $eÅ^{-3}$ to 0.437 $eÅ^{-3}$ respectively for the mentioned bonds, justifying the fact that the response of chemical bonds towards the external field depends on the position of the concerned bonds. The entire

spectrum of electron density $\rho_{bcp}(r)$ are posed in Table 1.

The Laplacian of electron density $[\nabla^2\rho_{bcp}(r)]$, is generated from the second order partial derivative operation on electron density confined to the three dimension grid, which quantifies the curvature of the function. The negative value of Laplacian directs to the locally concentrated charges at the bcp and a positive value leads to the locally depleted, indicating the strength of the chemical bonds **[8],** which plays vital role in the charge density distribution and strength **[9-10].** The Laplacian of the electron density examined for the W1and W2 nano wires indicated the ionic nature of the terminal bonds. The depleting nature of the Au(15)-S(14) bonding in W1 nano wire were effected from the presence of varying EF, exposed from the Laplacian values ranging from 2.942 eÅ^{-5} to 3.261 eÅ^{-5}, whereas the S(21)-Au(22) bond was found to be dropping the ionic nature with the increase of EF, which is evident from the Laplacian values for the concerned bonds (2.943 eÅ^{-5} to 2.825 eÅ^{-5}). The open shell interactions of the remining chemical bond were revealed from the Laplacian analysis exhibiting C(16)-C(9) / C(7)-C(8) bonds of the W1 molecule as the strongest bonds showing the Laplacian value of ~-20.279 eÅ^{-5}, which gradually reduces the covalent nature with increase of EF to 0.26 V (~ 19.7 eÅ^{-5}). The studies revealed the depleted nature of the C-S bonds, might due to the electro negativity of Sulphur atoms. Remarkably at the maximum electric field of 0.26 VÅ^{-1} ,the $\nabla^2\rho_{bcp}(r)$ value of S(21)-C(20) / S(23)-C(21) [W1/W2] increased from ~5 eÅ^{-5} to ~-11 eÅ^{-5}, illustrating the authenticity that the external EF can strengthen the chemical bonds. The nature of chemical bonds prevailed in the concerned molecules along with the variation in external field were tabulated in table 2.

Fig (6 a-6b) spectacles the dissimilarity of deformation and the Laplacian of electron density distribution for zero and various applied field. The deformation density map shows the quantity of electronic charges for the applied EF varying from 0 VÅ^{-1} to 0.26 VÅ^{-1}. The variations of the topological parameters were found to be equivlent but the extent of the effect for the external EF is found to be different. The graph clearly indicate that the presence of substituted Sulphur atom in the initial aromatic ring of W2 nanowire reduces the elctron density, strength of the bonds and the energy density.

3.3 ENERGY DENSITY

The total energy density H(r) of the molecule has been studied to investigate the bond strength. The positive laplacian value results in the control of the kinetic energy density, which contributes to the depletion of bond charge at the critical point of the bond; whereas the negative laplacian reflects the regulation of the potential energy density and the concentration of charges. The total energy density H(r) from the potential energy density V(r) can be equated with the local kinetic energy density G(r) in the bonding area as

H(r) = G(r) + V(r)[11].

The current study states that the G(r) is positive, V (r) is negative and the total energy density H(r) is negative, it is clear that in all cases V(r) is greater than G(r).

The negative total energy density H(**r**) for the associated bonds of the molecules (W1 and W2) reveals that the concentration of electrons in the bonding regions. The total energy density corelate with the nanowires exhibited values ~-2 HÅ^{-3}, indicating the covalent nature. Impressive results were observed in W2, where the substituted Sulphur atom in the aromatic ring reduces the energy density. The total energy density H(r) for C(13)-S(15) varied from -0.836 HÅ^{-3} to -0.827 HÅ^{-3}, where as the energy shifted from -0.833 HÅ^{-3} to -1.355 HÅ^{-3} for S(23)-C(21) bond, when the electric field applied to W2 wire increased from 0 VÅ^{-1} to 0.26 VÅ^{-1} .

The effect of varying electric field on the terminal AuS bonds is not identical as the field inc reases In general, it is known
asthe differences in energy density at both ends of the molecule are not equivalent. The total energy density associated with Au(15)-S(14) bond of W1 nanowire varied to an amount of ~0.1 HÅ^{-3} when the EF increased to 0 to 0.26 VÅ^{-1}. Where as ~0.04 HÅ^{-3} deviation can be observed in the neighboring bond [S(21)-Au(22)]. Similar trend for the terminal bonds were detected for the W2 wire. The values of energy density distribution of the molecule is listed in the table 3. The variation of the energy densities for W1 and W2 nanowires were compared in Fig. 7, to analyze the pattern in the variation.

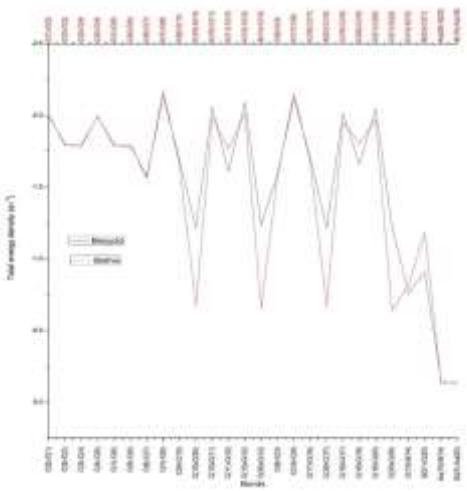

Fig 7 : The variation of energy density for W1 and W2 nano wire in varying electric field.

3.4 ATOMIC CHARGES

The fundamentals of charge distribution of atoms in molecule is vital to recognize the chemical reactivity, molecular electrostatic potential (MESP) and the electrostatic interactions [12,13]. The charge distribution of molecules has a significant contribution in calculating the electrical conductivity of a molecular system **[14]**. Thus, to reveal all the charge associated molecular properties, it is mandatory to analyze the redistributed charges of atoms under zero and higher applied electric field. Meanwhile different algorithms implement different methodology over the charge calculation [15-18]; it is a preliminary factor to calculate the electronic charges from various algorithms. Presently, the charge distribution for zero and higher bias determined by electrostatic potential fitting methods, which was compared against the natural population analysis (NPA) charges. Amongst, charges calculated from NPA scheme are superior pattern. Comparative plot on the effect on atomic charges due to the varying electric field is represented in Fig. 8.

The charges of C(3) and C(6) atoms derived from MPA scheme possesses high positive charge (0.51e). The MPA charge of terminal S-atom in the left end of W1 is 0.076e and it is increased by 0.1e when field increases. Unlikely, the corresponding charge of the right end S-atom was decreased from 0.08 to 0.05e with the applied electric field. The similar trend was observed for W2 molecular nanowire. Regarding Au atom, there is no significant changes in MPA charges was noticed in both the ends of W1 and W2 molecules. Whereas the NPA charge of Au atoms at the left end was decreased by 0.1e and increased by 0.2e at the right end when the electric field is increased from 0 to 0.26V/ Å. From the graph it is clearly evident that the redistribution of charges is systematic in the right and left region of the molecule.

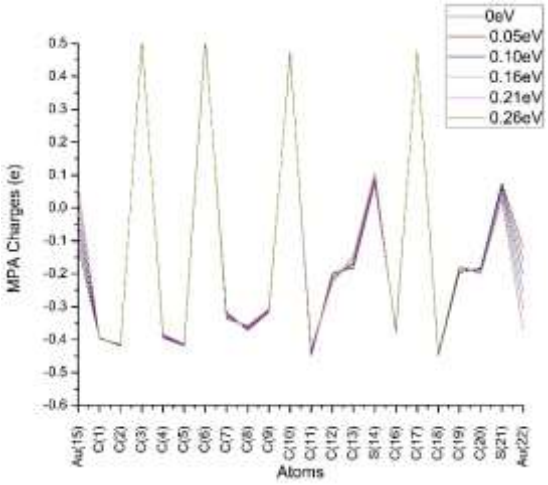

8(a)

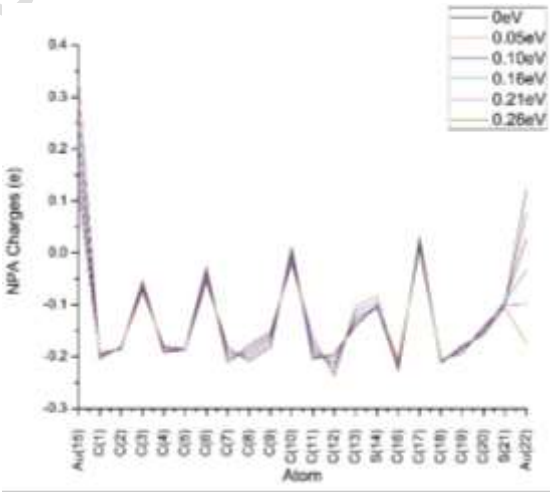

8(b)

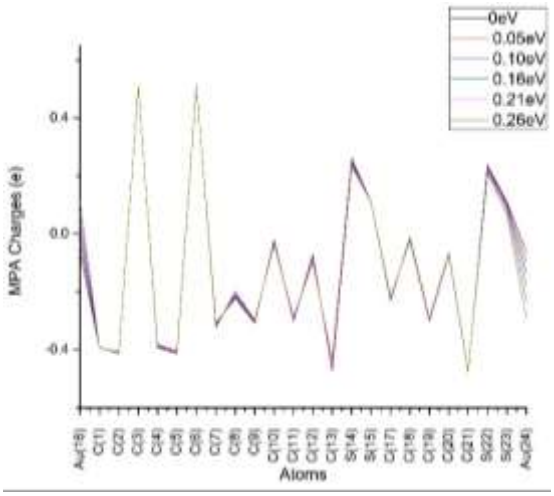

8(c)

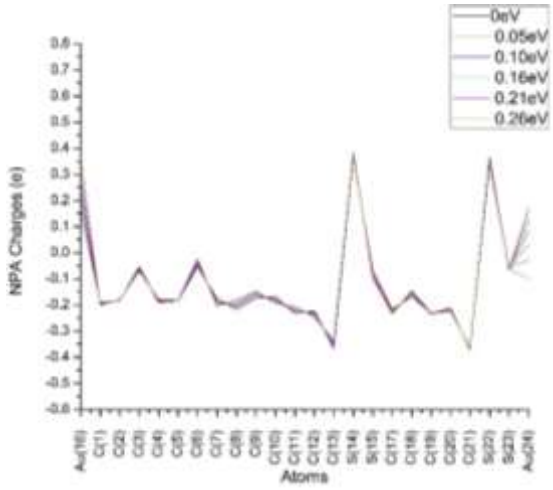

8(d)

Fig. 8(a-d) The variation of atomic charges for W1(8a,8b) and W2(8c,8d) nano wire in varying electric field.

3.5 FRONTIER MOLECULAR ORBITAL ANALYSIS

The energy difference between the highest molecular orbital occupied (HOMO) and the lowest unoccupied molecular orbital (LUMO) is referred to as the HOMO-LUMO gap (HLG),which plays vital role in the conducting properties of the nano wire [19]. Thus it is important to study the variations in the homo-lumo gap for the concerned molecule in varying electric field. Fig.(8) depicts the variation of HLG for the zero and non-zero bias of molecular wire.

The appliedelectric field illustrates the syst em's orbital frontier energy levels, which differ from oneanother and are primarily symmetrical for the re verse electric field.

The studies revealed that the increasing electric field allows the electrons to occupy the higher energy levels. It is evident from the variation of HLG from 1.655eV/1.772 eV to 0.882eV/0.836eV for [W1/W2] when the electric filed reaches 0.26 VÅ^{-1}from 0 VÅ^{-1}. Spectrum of density of state (DOS) has been plotted for the zero and non-zero applied electric field (Fig(9)) in which the hybridization of the molecular level broadens the DOS peaks with respect to the gold atom at both the ends of the molecule. The red and yellow line in the DOS spectrum specifies the HOMO and LUMO levels.

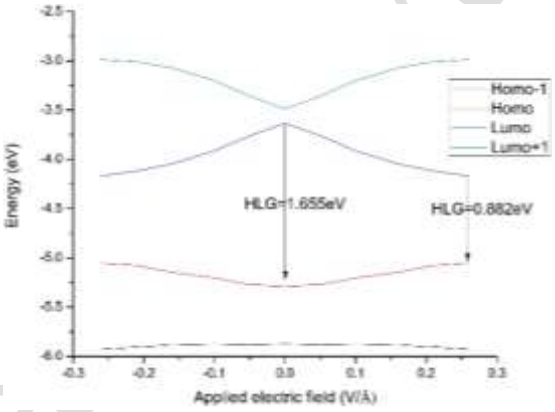

9(a)

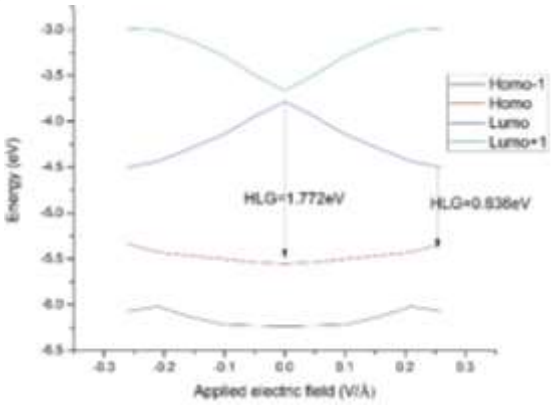

9(b)

Fig. 9 (a-b). Showing the variation of HLG for the various applied EFs in Au and S substituted W1 and W2 nanowire.

Fig. (10) elucidates the redistribution of the molecular orbital associated with the structures for the zero and higher applied electric fields . Rational shrinkage of the homo lumo energy gap is observed for both the nanowires, when the electric field is increased from 0 to 0.26 VÅ^{-1}. The calculated energy shows that the electrons occupied at the outermost energy level can be

excited to the higher energy levels at LUMO through infrared radiations when the target is subjected to an electric field of 0.26 VÅ^{-1}, while the radiations at the visible region can excite the valance electrons in the absence of external field, indicating the concerned nanowire can exhibit optical properties.

3.6 ELECTROSTATIC POTENTIAL

Gadre and colleagues[20,21] earlier reported that the Electrostatic Potential IsoSurface Plotting (ESP) topography is a succinct way of investigating a molecule's chemical reactivity and electrostatic properties. The polar nature of the molecule can be easily identified from the plot, which plays important role in the crystallization process.

Fig. (12) displays the three dimensional isosurface representations of electrostatic potential for the nanowires under study under zero and non-zero bias. Here, blue region denotes positive potential and red region symbolizes negative potential. The surface potential obviously replicates the opposing influences from the nuclei and the electrons, therefore it highly portraited the charged sections of the molecule [22].

The surface is found to be positive all over the backbone of the molecule for the zero applied electric field; this positive influence is qualified from the nuclei. While, the negative potential is pivoted over Sulphur atoms present at right and left ends of the molecule; the effect of the external field on the polar nature is identified as the electronegative region at the left side of W1 and W2 nano wires diminishes as the field reaches 0.26 VÅ^{-1} , and the molecule became bipolar. Further, the balance parameter [23] was calculated for W1 and W2 molecules to explicit the exact composition of positive and negative potential. The balance parameter reaches a maximum value 0.25, when $\sigma^2(+) = \sigma^2(-)$. Here, we have calculated the positive and negative electrostatic potential variances and the electrostatic balance parameter listed in table 4 and the variation of balance parameter with the electric fields are shown in the fig.13

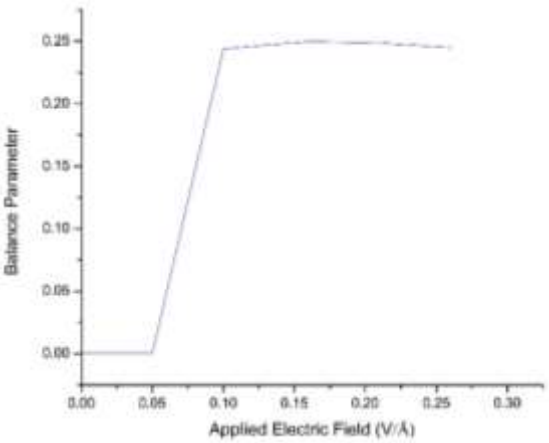

13(a)

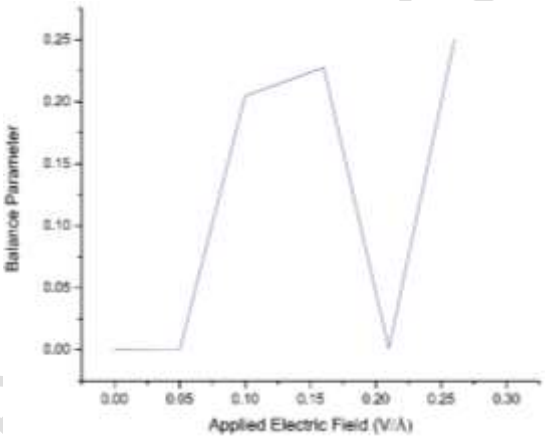

13(b)

Fig. 13(a)-13(b) The variation of balance parameter for W1 and W2 nanowires in varying electric field

3.7 I-V RELATION AND MOLECULAR POLARIZATION

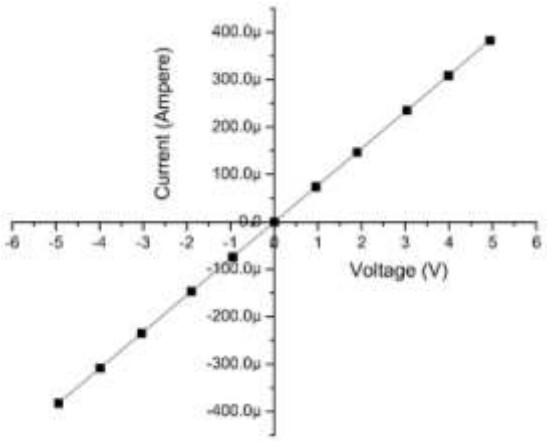

14(a)

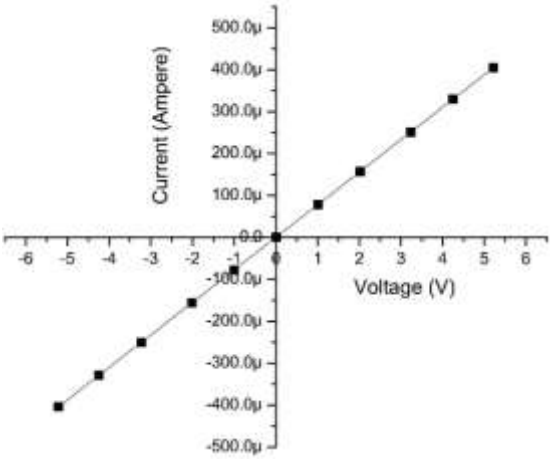

14(b)

Fig. 14(a)-14(b) **I-V** characteristics plot of Au and S substitute (a) W1 and (b) W2 for the zero and various applied EF

The characteristic curve of current/voltage (IV) co mmonly used to assess the working of electric components in circuits [24]. The Au and S substituted nanowires characteristic I- V plot (fig (14)) shows the linear dependence of the increasing bias voltage with the current indicating the wire offers only small resistance to the charge.

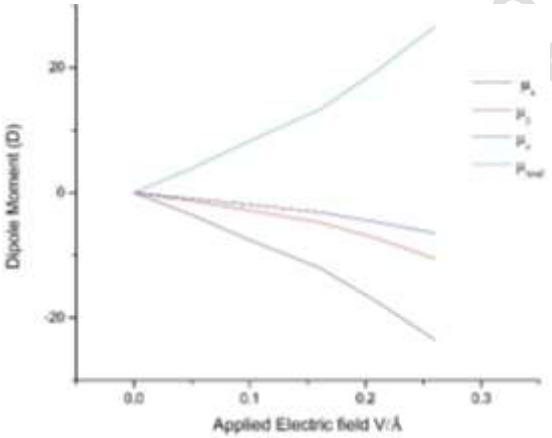

15(a)

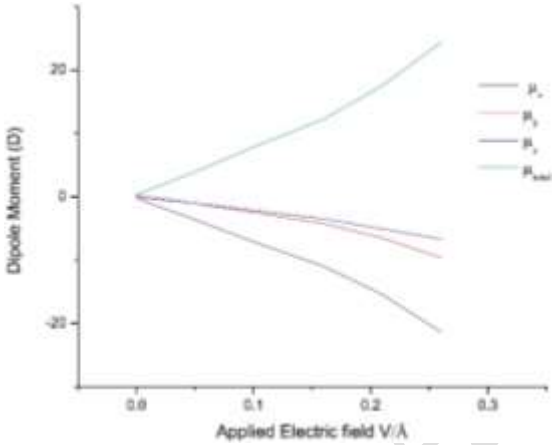

15(b)

Fig 15(a-b) Molecular dipole moment of Au and S substituted (a) W1 and (b) W2

The polarization of the concerned molecule by the external EF field develop a the dipole moment in the molecule that measures the polarity [25] of the nano wire found to be varying with respect to the external field. The variations of molecular dipole moment for the various applied EF were analyzed by Kirtman et al and found almost linear in nature. The Fig. 15 shows the variation of x, y and z components of dipole moment (μ_x, μ_y, and μ_z) and the resultant molecular dipole moment (μ) for various applied EFs, the large variation of x-component may be due to the application of field along x-direction.

4. CONCLUSION

The variation of the electron density and the electrostatic aspect of the W1 and W2 nano wire in varying electric field were studied in detail incorporating the DFT calculations and QTAIM analysis. Irregular effects on the topological parameters and the electrostatic characteristics of both molecules were observed in the research, exposing the geometric position of the chemical bonds possess vital role in the effect of the external electric field. The stability and the strength of the terminal bonds were found to be fluctuating from 0.494 $eÅ^{-3}$ to 0.522 $eÅ^{-3}$ while contrary result observed in the similar bond on the inverse opposite position, justifying the effect of the external EF on the nanowire depends on the geometric position of the atoms. Identical comparisons were observed in the Laplacian of electron density. The research resolved the excitation of the electrons from the valance orbitals from the reduction of the homo lumo energy gap from 1.65eV/1.722eV to

0.883eV/0.836eV by virtue of the increasing applied external electric field. The studies proved the conducting nature of the nanowires from the linear IV characteristics along with the diminishing electrostatic positive potential on the terminals with increasing electric field. Complementary results of the examination may consent to design the electronic gadgets at nanometric scale by utilizing polycyclic hydrocarbon nanowires of suitable characters

REFERENCES

1. Talapin, D. V., Lee, J. S., Kovalenko, M. V. & Shevchenko, E. V. Prospects of Colloidal Nanocrystals for Electronic and Optoelectronic Applications. Chem. Rev. 110, (2010): 389–458
2. J. Jiu and K. Suganuma, "Metallic Nanowires and Their Application," in IEEE Transactions on Components, Packaging and Manufacturing Technology,vol.6,no.12 (2016): 1733-1751.
3. Frisch M J, Trucks G W, Schlegel H B, Scuseria G E, Robb M A, Cheeseman J R, Montgomery J A, Jr Vreven T, Kudin K N, Burant J C, Millam J M, Iyengar S S, Tomasi J, Barone V, Mennucci B, Cossi M,Scalmani G, Rega N, Petersson G A, Nakatsuji H, M. Hada, Ehara M, Toyota K, Fukuda R, Hasegawa J, Ishida M, Nakajima T, Honda Y, Kitao O, Nakai H, Klene M, X. Li, Knox J E, Hratchian H P, Cross J B, Adamo C, Jaramillo J, Gomperts R, Stratmann R E, Yazyev O, Austin A J, Cammi R, Pomelli C, Ochterski J W, Ayala P Y, Morokuma K, Voth G A, Salvador P, Dannenberg J J, Zakrzewski V G, Dapprich S, Daniels A D, Strain M C, Farkas O, Malick D K, Rabuck A D, Raghavachari K, Foresman J B,Ortiz J V, Cui Q, Baboul A G, Clifford S, Cioslowski J, Stefanov B, G. Liu, A. Liashenko, Piskorz P, Komaromi I, Martin R L, Fox D J, Keith T, Al- Laham M A, Peng C Y, Nanayakkara A, Challacombe M, Gill P M W, B. 47 Johnson, Chen W, Wong M W, Gonzalez C, Pople J A, Gaussian Inc Pittsburgh P A, (2003).
4. A. D. Becke. "Density-functional exchange-energy approximation with correct asymptotic behavior". Phys. Rev. A. 38 (6) (1988): 3098–3100
5. Bader R F W, Atoms in molecules - A quantum theory, Clarendon Press, Oxford 1990; Biegler-Konig F W, Cheeseman J, Keith T A, Bader R F W, AIMPAC Program Package, McMaster University, Hamilton, Ontario, 1992; Bader R F W, Tang T H, J Comput Chem 3 (1982): 317-328.
6. Boyle N O, GaussSum, Revision 2.1, (2007)
7. Bader R F W, J Chem Phys 73 (1980):2871-2883.
8. D. Cremer and E. Kraka, "A description of the chemical bond in terms of local properties of electron density and energy, in conceptual approaches in quantum chemistry—models and applications," Croatia Chemica Acta, vol. 57 (1984): 1259–1281.
9. V. R. Hathwar, A. K. Paul, S. Natarajan, and T. N. Guru Row, "Charge density analysis of a pentaborate ion in an ammonium borate: toward the understanding of topological features in borate minerals," Journal of Physical Chemistry A, vol. 115, no. 45, (2011): 12818–12825.
10. R. F. W. Bader and H. Essen, "The characterization of atomic interactions," The Journal of Chemical Physics, vol. 80, (1984):1943-1960.
11. Anbu V., Vijayalakshmi K.A., Karunathan R., Stephen A.D., Nidhin P.V. Arab J Chem.,12 (2019):621-632.
12. Mishra P C, Kumar A, Murray J S, Sen K D (Eds.), Theoretical and Computational Chemistry Book Series, 3, Elsevier, Amsterdam, (1996)
13. Volkov V, Gatti C, Abramov Y, Coppens P, Acta Crystallogr A 56 (2000): 252
14. Maciel G S, Garcia E, Chem Phys Lett 409 (2005):29-33.
15. Martin F, Zipse H, J Comput Chem 26 (2005):97-105.
16. Bultinck P, Langenaeker W, Lahorte P, De Proft F, Geerlings P, Van Alsenoy C, Tollenaere J P, J Phys Chem A 106 (2002):7895-7901.
17. Breneman C M, Wiberg K B, J Comp Chem (1990) 11:361-373
18. Reed R A, Curtiss L A, Weinhold F, Chem Rev (1988) 88:899-926.

19. Chamani, Z. & Bayat, Zakiyeh & Mahdizadeh, Sayyed Jalil. Theoretical study of the electronic conduction through organic nanowires. J Struct Chem. 55 (2014): 530-538.
20. Gadre S R, Pathak R K, Proc Indian Acad Sci Chem Sci 102 (1990):189-192; S.R. Gadre S R, Babu K, Rendell A P, J Phys Chem A104 (2000):8976-8982.
21. Gadre S R, Shirsat R N, Electrostatics of Atoms and Molecules, Universities Press: Hyderabad, 2000; Gadre S R, Computational Chemistry: Reviews of Current Trends Lesczynski, J. Ed., World Scientific: Singapore, 4,2000.
22. Kulkarni A D, Babu K, Gadre S R, Bartolotti L J, J Phys Chem A 108 (2004):2492-2498.
23. J.S. Murray, P. Politzer, Statistical analysis of the molecular surface electrostatic potential: An approach to describing noncovalent interactions in condensed phases, J. Mol. Struct. THEOCHEM. (1998): 107-114.
24. H. J. van der Bijl "Theory and Operating Characteristics of the Themionic Amplifier". Proceedings of the IRE. Institute of Radio Engineers. 7 (2) (1919): 97–126
25. Raymond A. Serway; John W. Jewett Jr. Physics for Scientists and Engineers, Volume 2 (8th ed.). Cengage Learning. (2009): 756–757.

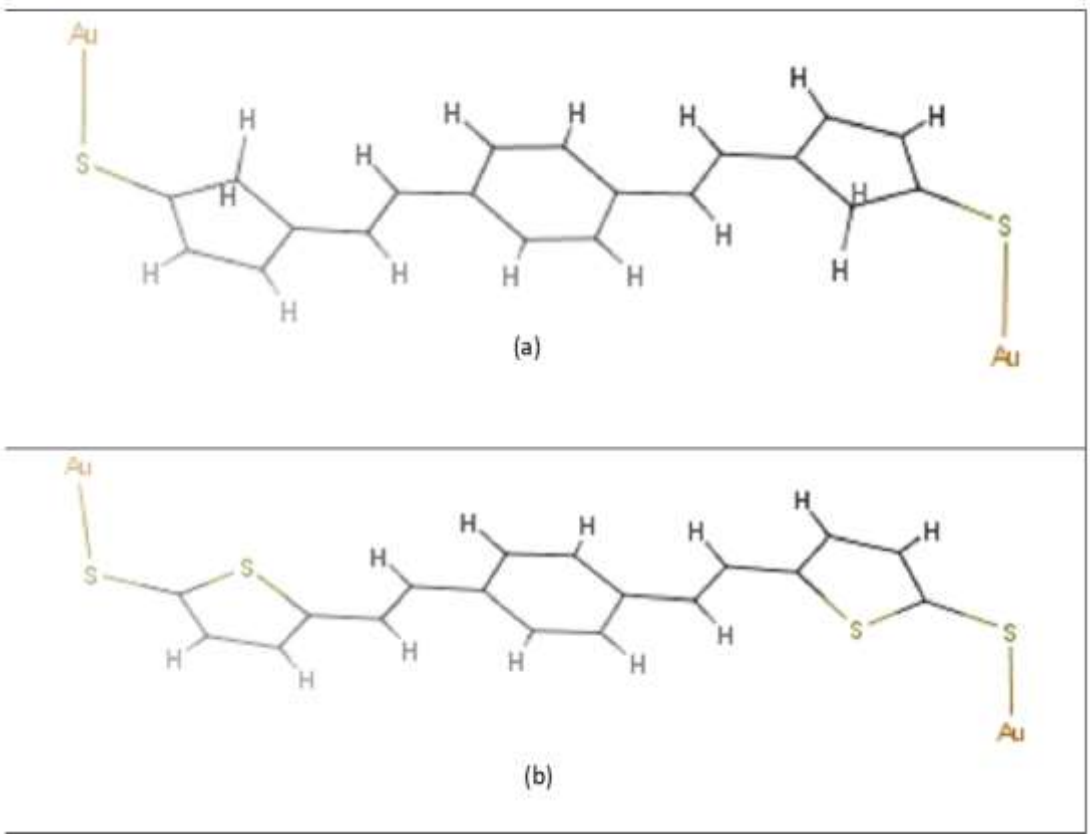

Fig. 1. Schematic diagram of (a) W1 and (b) W2 fused with Sulpher and Gold atoms

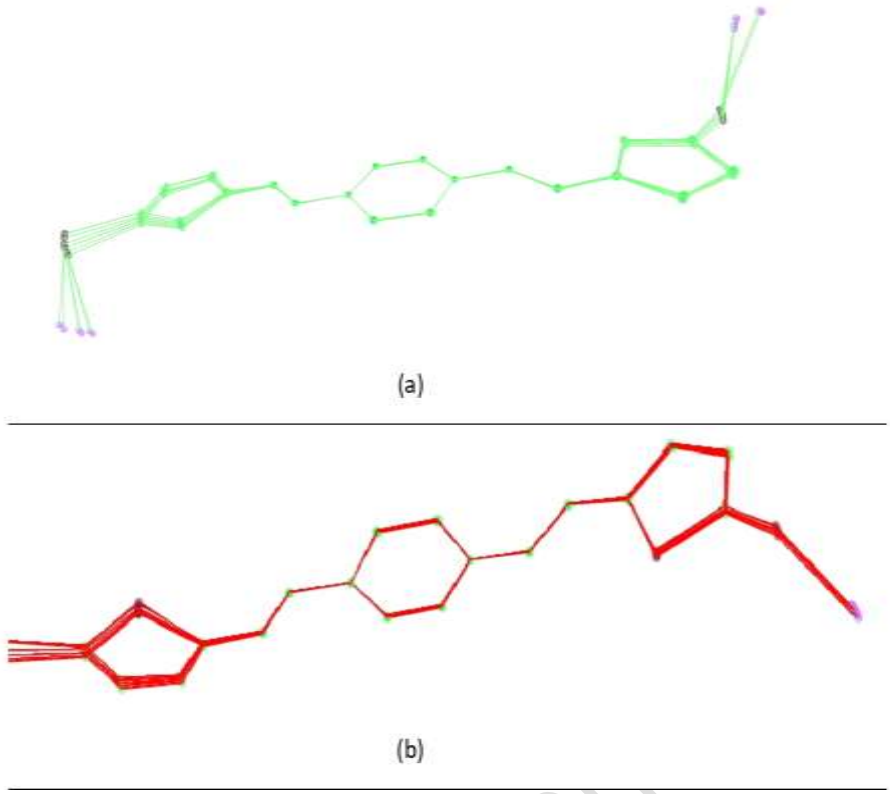

Fig. 2 Superimpose of the Au & S substituted (a) W1 and (b) W2 for the zero and various applied EFs.

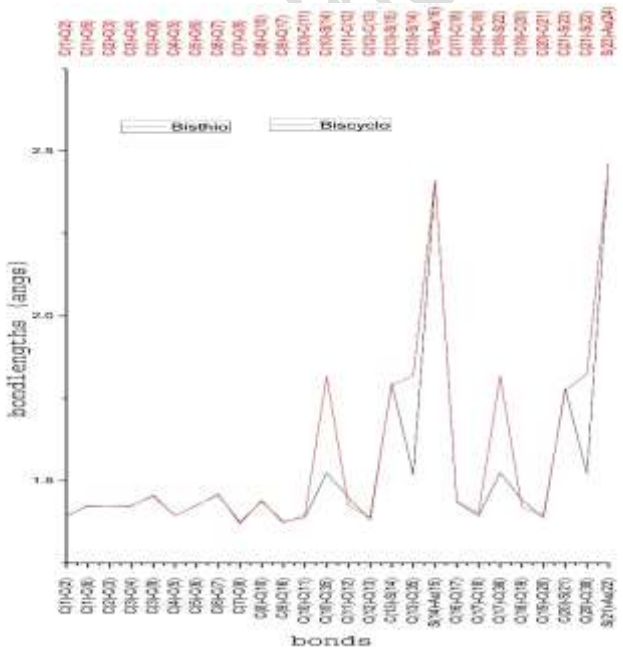

Fig. 3 Variation of average bond length of W1 and W2 molecule.

Vol 11, Issue 5,May/ 2020
ISSN NO: 0377-9254

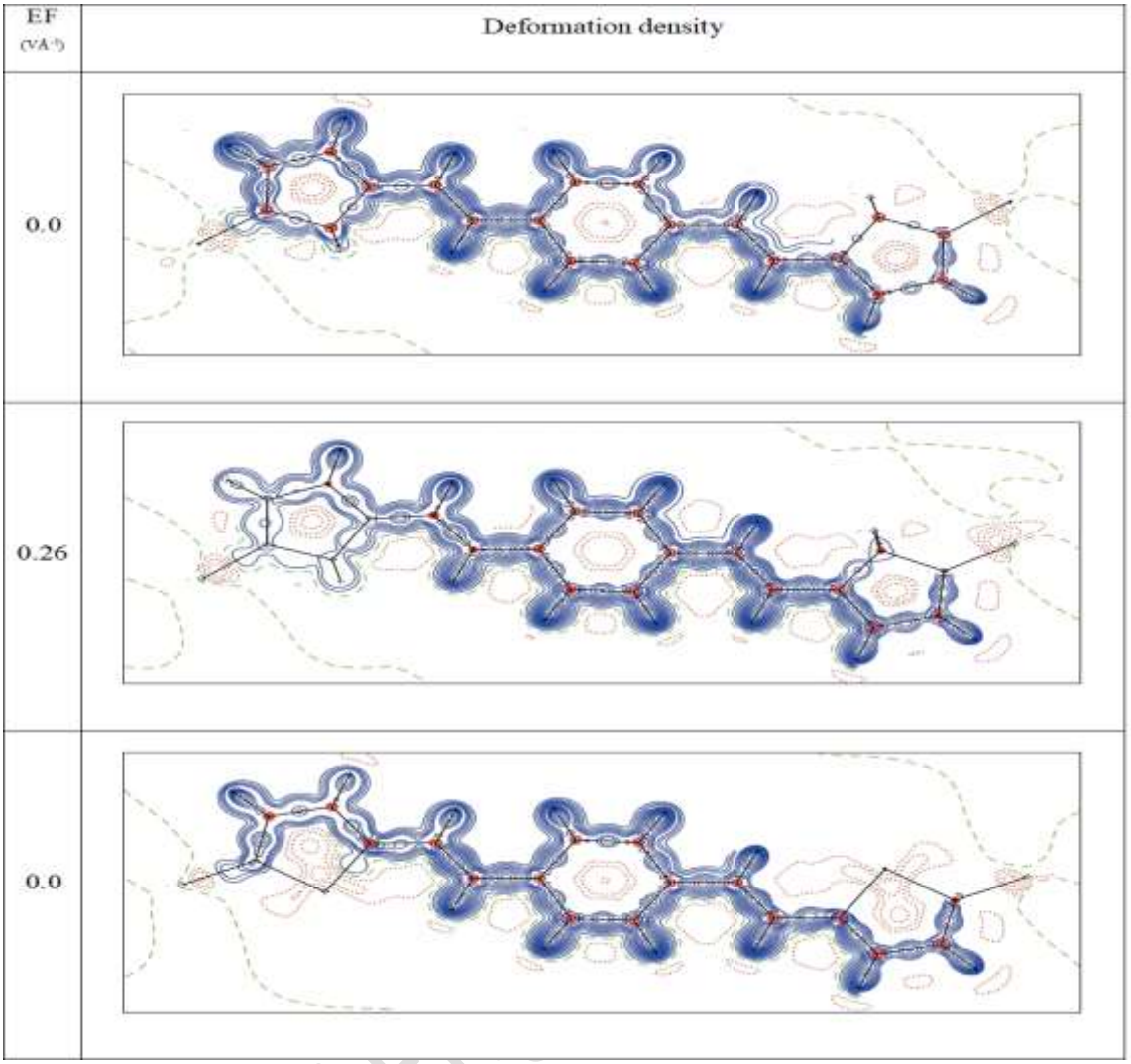

Fig. 4. Deformation density map plotted for molecular plane of (a) W1 and (b) W2 for the zero and 0.26 applied EFs. Solid lines represent positive contours, dotted lines are negative contours and dashed lines are zero contours. The contours are drawn at 0.05 eÅ-3 intervals

Vol 11, Issue 5,May/ 2020
ISSN NO: 0377-9254

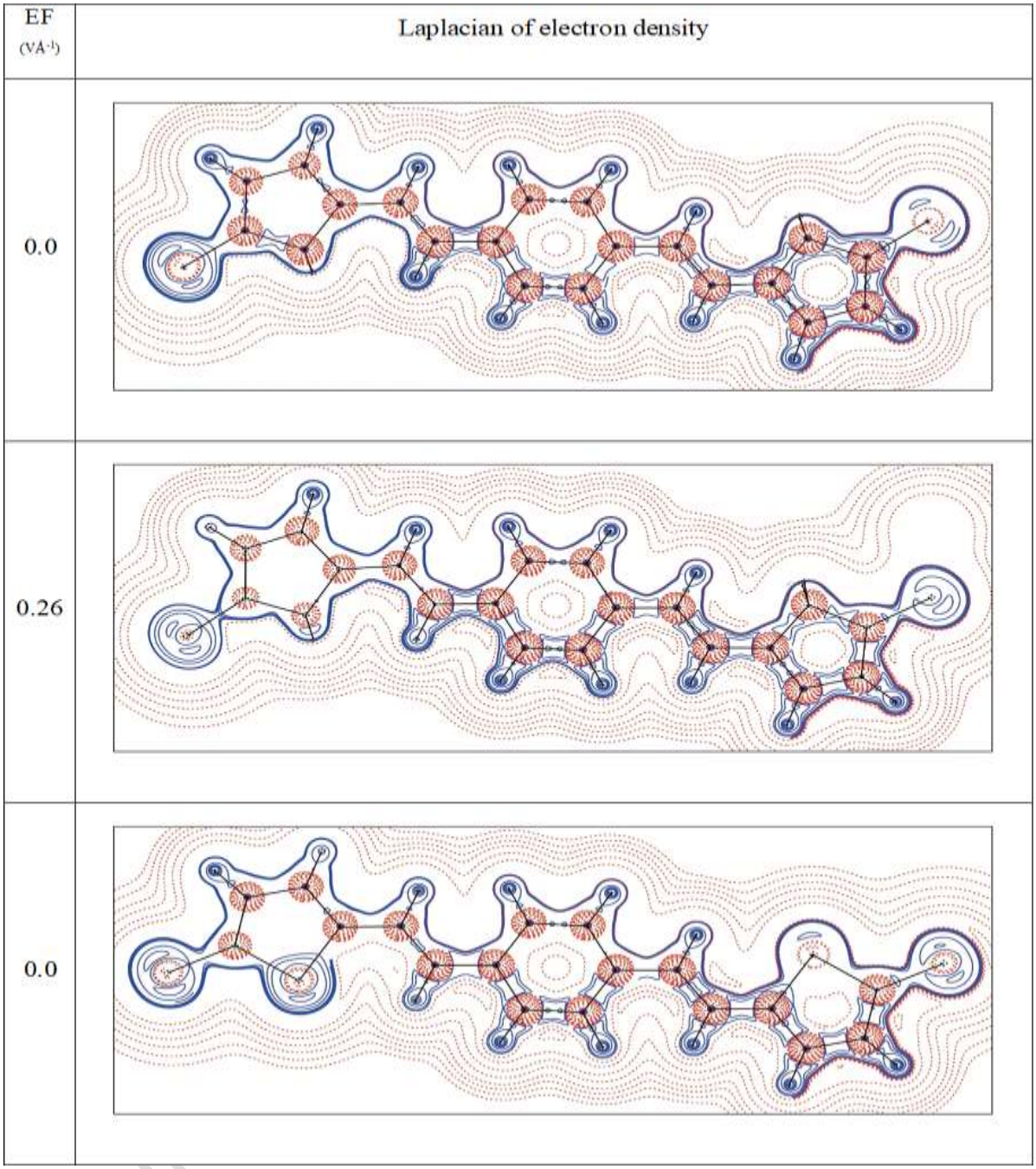

Fig. 5 Laplacian of electron density map plotted for molecular plane of (a) W1 and (b) W2 for the zero and 0.26 applied EFs.The contours are drawn in logarithmic scale, $3x2^{N}$ eÅ^{-5}, where N = 2, 4 and $8x10^{n}$, n= -2, -1, 0, 1, 2. Solid lines are positive contours and dotted lines are negative contours

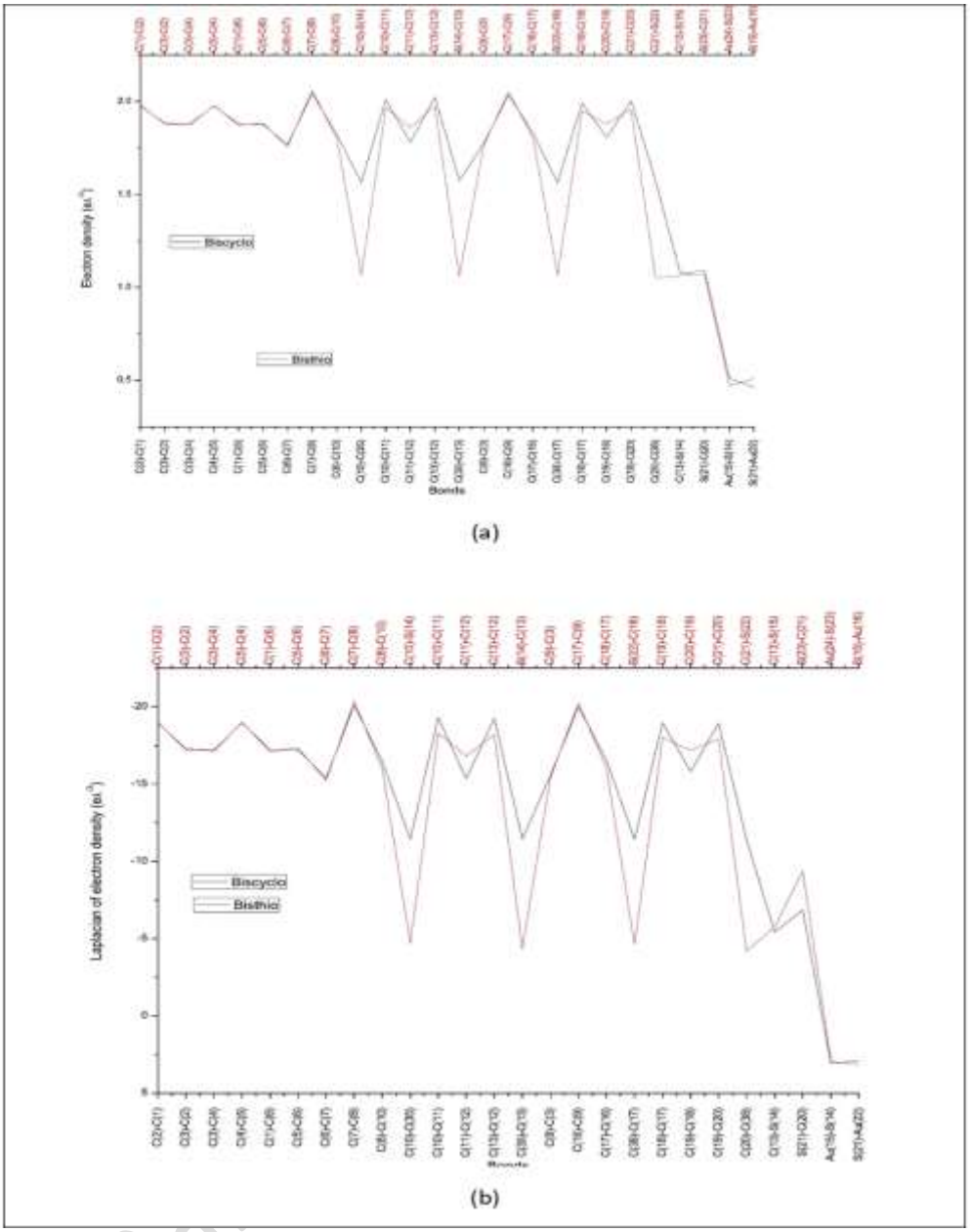

Fig. 6 a- 6b Showing the variations of $\rho_{bcp}(r)$ and the Laplacian of electron density values of Au and S substituted W1 and W2 for zero and various applied EFs.

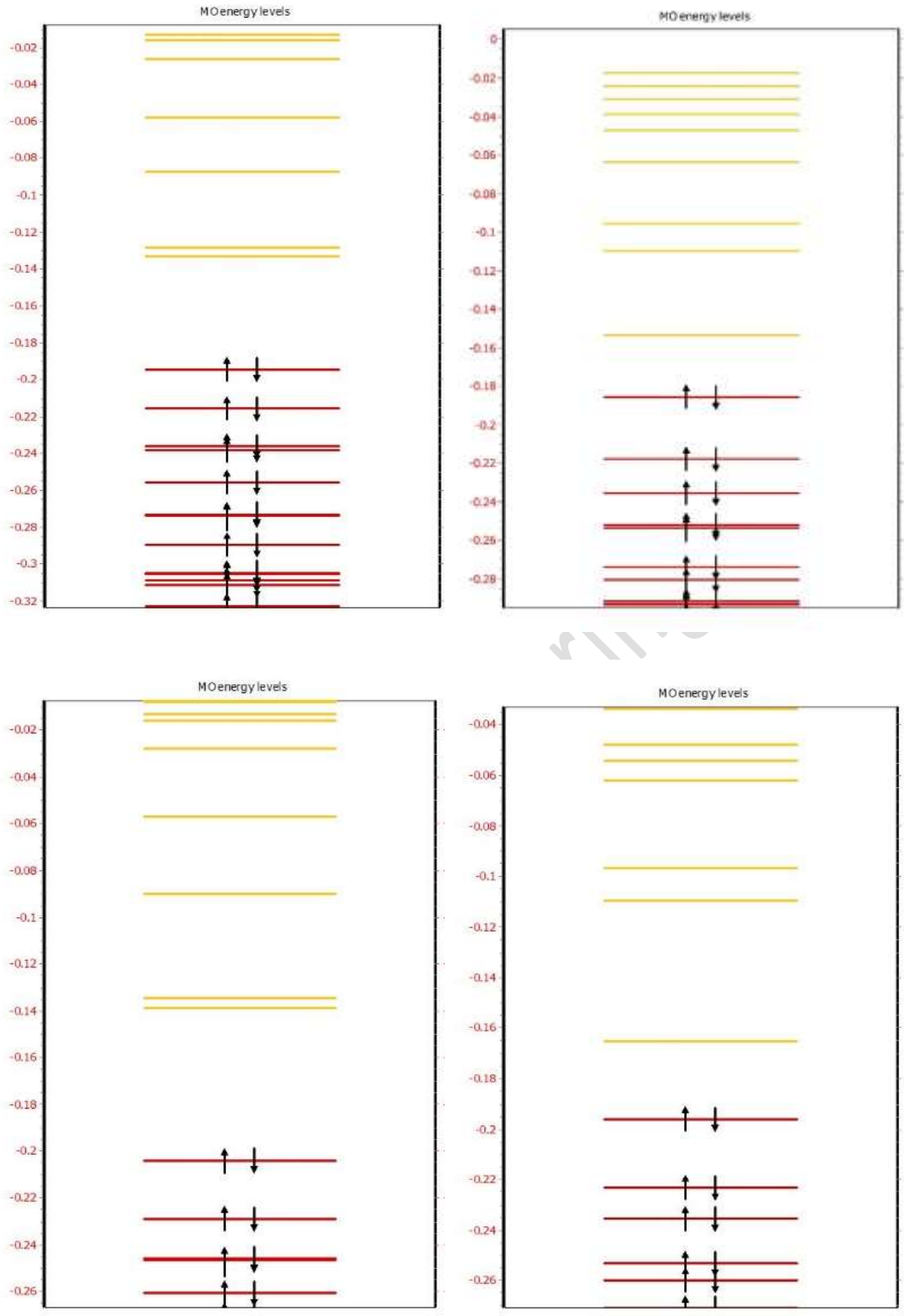

Fig 10: MO energy level of (a)W1 and (b) W2 for 0 and 0.26eV

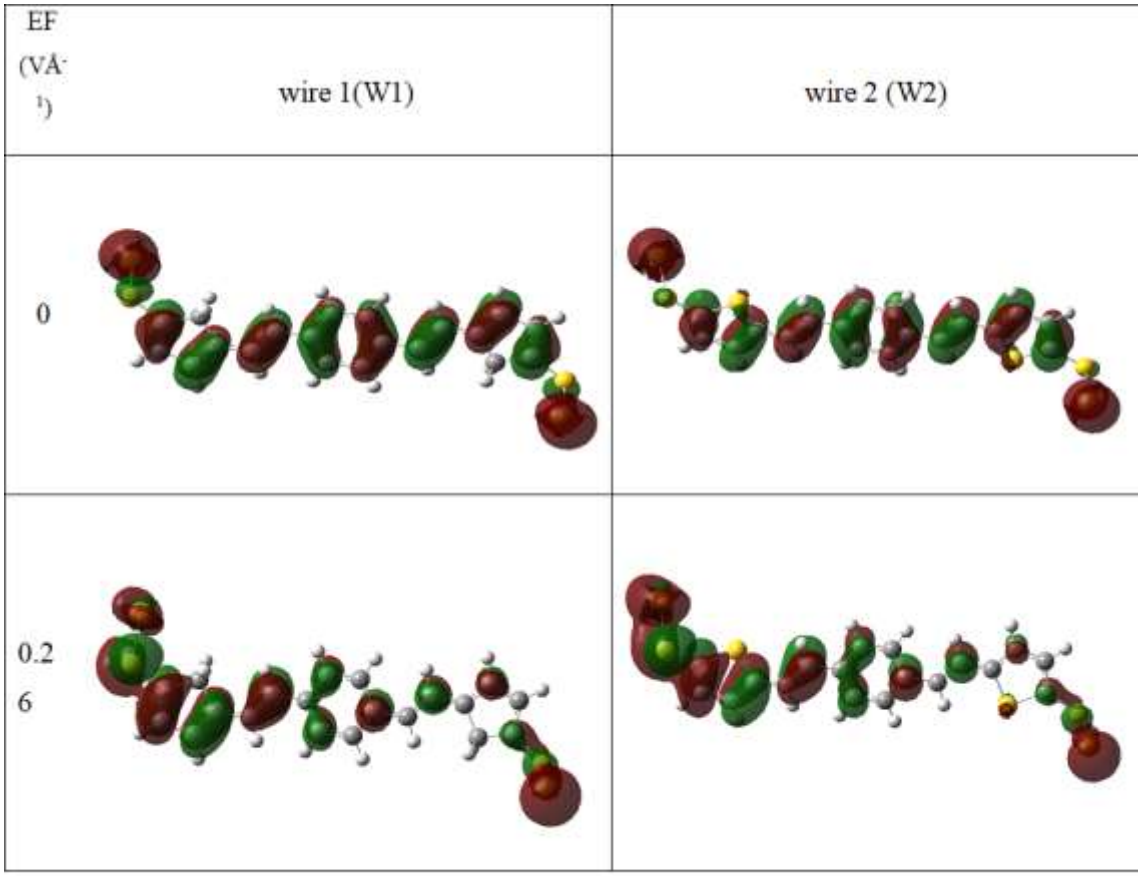

(a)

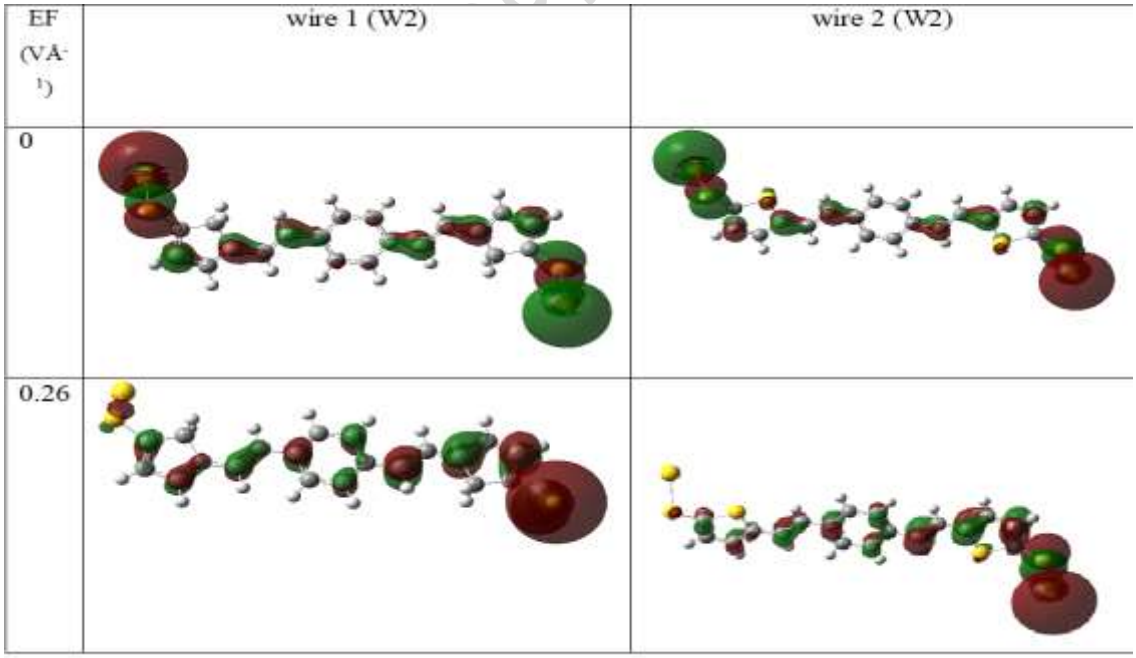

(b)

Fig. 11(a) – 11(b) Isosurface representation of molecular orbitals (HOMO, LUMO) W1 and W2 for the zero and various applied EFs, which are drawn at 0.05au surface values.

Vol 11, Issue 5,May/ 2020
ISSN NO: 0377-9254

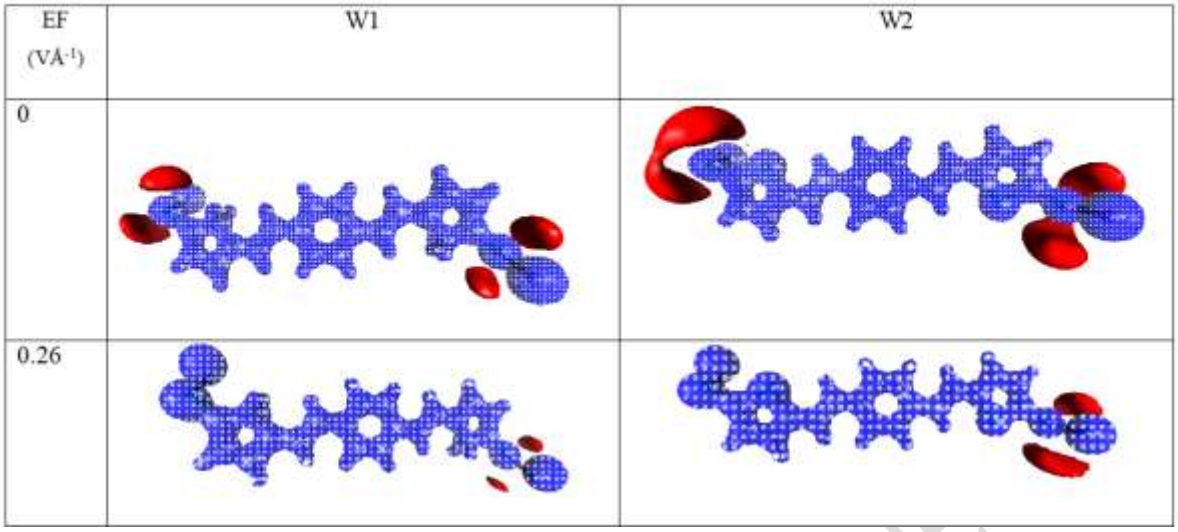

Fig. 12 Isosurface representation of ESP of Au and S subsitituted W1 and W2 for EFs 0 and 0.26eV. Blue: positive potential (0.5 eÅ^{-1}), Red: negative potential (-0.04 eÅ^{-1}).

Table 1 Electron density $\rho_{bcp}(r)$ (eÅ^{-3}) values of the Au and S substituted W1 and W2 for the zero and various applied EFs (VÅ^{-1}).

wire 1 (W1)

Bonds	0	0.05	0.10	0.16	0.21	0.26
C(2)-C(1)	1.971	1.972	1.974	1.978	1.984	1.991
C(3)-C(2)	1.886	1.886	1.883	1.879	1.873	1.866
C(3)-C(4)	1.882	1.881	1.879	1.874	1.867	1.86
C(4)-C(5)	1.971	1.972	1.974	1.978	1.982	1.987
C(1)-C(6)	1.882	1.881	1.878	1.873	1.866	1.858
C(5)-C(6)	1.886	1.885	1.882	1.877	1.871	1.863
C(6)-C(7)	1.754	1.753	1.757	1.764	1.775	1.789
C(7)-C(8)	2.054	2.054	2.051	2.045	2.033	2.02
C(8)-C(10)	1.811	1.81	1.814	1.821	1.834	1.849
C(10)-C(35)	1.565	1.566	1.564	1.564	1.562	1.56
C(10)-C(11)	2.013	2.016	2.017	2.014	2.007	1.995
C(11)-C(12)	1.777	1.772	1.769	1.774	1.785	1.802
C(13)-C(12)	2.026	2.031	2.031	2.028	2.019	2.006
C(35)-C(13)	1.576	1.576	1.575	1.574	1.571	1.569
C(9)-C(3)	1.754	1.759	1.767	1.778	1.792	1.807
C(16)-C(9)	2.054	2.051	2.044	2.035	2.023	2.01

C(17)-C(16)	1.811	1.815	1.822	1.832	1.844	1.857
C(38)-C(17)	1.565	1.565	1.564	1.563	1.563	1.561
C(18)-C(17)	2.013	2.007	1.998	1.988	1.975	1.962
C(19)-C(18)	1.777	1.785	1.797	1.81	1.826	1.842
C(19)-C(20)	2.026	2.019	2.01	2	1.988	1.974
C(20)-C(38)	1.576	1.576	1.575	1.573	1.57	1.566
C(13)-S(14)	1.081	1.075	1.072	1.07	1.073	1.079
S(21)-C(20)	1.081	1.088	1.096	1.104	1.109	1.063
Au(15)-S(14)	0.494	0.501	0.51	0.514	0.519	0.522
S(21)-Au(22)	0.494	0.486	0.475	0.461	0.442	0.421

wire 2 (W2)

Bonds	0	0.05	0.10	0.16	0.21	0.26
C(1)-C(2)	1.97	1.97	1.972	1.975	1.98	1.987
C(3)-C(2)	1.889	1.889	1.887	1.883	1.878	1.872
C(3)-C(4)	1.885	1.884	1.882	1.878	1.872	1.866
C(5)-C(4)	1.97	1.971	1.973	1.976	1.98	1.985
C(1)-C(6)	1.885	1.884	1.882	1.878	1.873	1.865
C(5)-C(6)	1.889	1.888	1.886	1.882	1.877	1.87
C(6)-C(7)	1.749	1.748	1.75	1.756	1.765	1.778
C(7)-C(8)	2.066	2.067	2.065	2.061	2.053	2.04
C(8)-C(10)	1.794	1.793	1.795	1.801	1.811	1.826
C(10)-S(14)	1.069	1.069	1.069	1.068	1.067	1.062
C(10)-C(11)	1.965	1.969	1.97	1.968	1.964	1.957
C(11)-C(12)	1.861	1.855	1.854	1.855	1.86	1.871
C(13)-C(12)	1.974	1.977	1.979	1.978	1.974	1.962
S(14)-C(13)	1.057	1.059	1.061	1.062	1.064	1.066
C(9)-C(3)	1.749	1.753	1.76	1.77	1.782	1.796
C(17)-C(9)	2.066	2.063	2.057	2.049	2.039	2.028
C(18)-C(17)	1.793	1.797	1.803	1.811	1.821	1.832
S(22)-C(18)	1.07	1.069	1.067	1.066	1.063	1.06

C(19)-C(18)	1.965	1.96	1.954	1.946	1.937	1.928
C(20)-C(19)	1.861	1.866	1.874	1.883	1.893	1.902
C(21)-C(20)	1.974	1.969	1.962	1.954	1.945	1.935
C(21)-S(22)	1.057	1.055	1.052	1.049	1.046	1.042
C(13)-S(15)	1.077	1.069	1.064	1.059	1.055	1.058
S(23)-C(21)	1.076	1.083	1.058	1.06	1.061	1.06
Au(24)-S(23)	0.497	0.49	0.481	0.47	0.456	0.437
S(15)-Au(16)	0.501	0.506	0.51	0.512	0.513	0.516

Table 2 Laplacian of electron density $\nabla^2\rho_{bcp}(r)$ ($eÅ^{-5}$) values of Au and S substituted W1 and W2 for the zero and various applied EFs ($VÅ^{-1}$).

Wire1 (W1)

Bonds	**0**	**0.05**	**0.10**	**0.16**	**0.21**	**0.26**
C(2)-C(1)	-18.862	-18.875	-18.913	-18.987	-19.086	-19.206
C(3)-C(2)	-17.346	-17.332	-17.289	-17.219	-17.122	-17.007
C(3)-C(4)	-17.266	-17.252	-17.204	-17.13	-17.021	-16.897
C(4)-C(5)	-18.862	-18.879	-18.923	-18.986	-19.065	-19.15
C(1)-C(6)	-17.266	-17.25	-17.196	-17.115	-16.994	-16.859
C(5)-C(6)	-17.346	-17.331	-17.283	-17.209	-17.1	-16.973
C(6)-C(7)	-15.195	-15.175	-15.224	-15.341	-15.526	-15.75
C(7)-C(8)	-20.279	-20.283	-20.226	-20.12	-19.934	-19.716
C(8)-C(10)	-16.248	-16.244	-16.31	-16.443	-16.662	-16.92
C(10)-C(35)	-11.449	-11.451	-11.431	-11.421	-11.39	-11.363
C(10)-C(11)	-19.329	-19.385	-19.405	-19.36	-19.247	-19.067
C(11)-C(12)	-15.294	-15.201	-15.163	-15.236	-15.439	-15.747
C(13)-C(12)	-19.33	-19.402	-19.397	-19.358	-19.183	-18.966
C(35)-C(13)	-11.473	-11.476	-11.472	-11.454	-11.414	-11.377
C(9)-C(3)	-15.195	-15.276	-15.418	-15.614	-15.844	-16.093
C(16)-C(9)	-20.279	-20.227	-20.122	-19.974	-19.776	-19.555
C(17)-C(16)	-16.248	-16.311	-16.428	-16.59	-16.782	-16.989
C(38)-C(17)	-11.448	-11.441	-11.429	-11.412	-11.407	-11.374
C(18)-C(17)	-19.329	-19.232	-19.095	-18.922	-18.712	-18.495

C(19)-C(18)	-15.294	-15.447	-15.646	-15.885	-16.17	-16.439
C(19)-C(20)	-19.33	-19.219	-19.069	-18.888	-18.689	-18.452
C(20)-C(38)	-11.473	-11.466	-11.449	-11.424	-11.354	-11.295
C(13)-S(14)	-5.505	-5.386	-5.336	-5.318	-5.407	-5.57
S(21)-C(20)	-5.504	-5.668	-5.88	-6.152	-6.484	-11.369
Au(15)-S(14)	2.942	2.971	3.031	3.081	3.164	3.261
S(21)-Au(22)	2.943	2.919	2.907	2.889	2.856	2.825

wire 2 (W2)

Bonds	**0**	**0.05**	**0.10**	**0.16**	**0.21**	**0.26**
C(1)-C(2)	-18.855	-18.85	-18.878	-18.936	-19.022	-19.136
C(3)-C(2)	-17.403	-17.389	-17.355	-17.293	-17.208	-17.102
C(3)-C(4)	-17.317	-17.301	-17.26	-17.194	-17.105	-16.993
C(5)-C(4)	-18.847	-18.869	-18.904	-18.964	-19.041	-19.122
C(1)-C(6)	-17.315	-17.305	-17.27	-17.206	-17.115	-16.99
C(5)-C(6)	-17.403	-17.393	-17.361	-17.301	-17.215	-17.097
C(6)-C(7)	-15.113	-15.094	-15.121	-15.214	-15.368	-15.579
C(7)-C(8)	-20.479	-20.484	-20.451	-20.373	-20.246	-20.038
C(8)-C(10)	-15.828	-15.826	-15.875	-15.983	-16.154	-16.425
C(10)-S(14)	-4.712	-4.707	-4.715	-4.716	-4.708	-4.632
C(10)-C(11)	-18.266	-18.332	-18.352	-18.332	-18.268	-18.171
C(11)-C(12)	-16.83	-16.724	-16.698	-16.724	-16.814	-16.997
C(13)-C(12)	-18.2	-18.253	-18.271	-18.254	-18.191	-18.004
S(14)-C(13)	-4.296	-4.334	-4.349	-4.363	-4.379	-4.43
C(9)-C(3)	-15.115	-15.185	-15.307	-15.479	-15.688	-15.915
C(17)-C(9)	-20.474	-20.422	-20.336	-20.21	-20.051	-19.861
C(18)-C(17)	-15.825	-15.87	-15.957	-16.088	-16.25	-16.428
S(22)-C(18)	-4.713	-4.693	-4.67	-4.641	-4.603	-4.551
C(19)-C(18)	-18.265	-18.193	-18.092	-17.967	-17.827	-17.681
C(20)-C(19)	-16.823	-16.922	-17.056	-17.216	-17.39	-17.561
C(21)-C(20)	-18.197	-18.121	-18.019	-17.892	-17.744	-17.576
C(21)-S(22)	-4.3	-4.271	-4.234	-4.186	-4.127	-4.057
C(13)-S(15)	-6.002	-5.787	-5.678	-5.618	-5.628	-5.795

S(23)-C(21)	-5.977	-6.253	-10.975	-11.024	-11.033	-10.989
Au(24)-S(23)	2.991	2.964	2.944	2.927	2.911	2.891
S(15)-Au(16)	3.019	3.051	3.098	3.145	3.198	3.304

Table 3 Bond energy density ($HÅ^{-3}$) values of Au and S substituted W1 and W2 molecule for the zero and various applied EFs ($VÅ^{-1}$).

Wire 1 (W1)

Bonds	**0**	**0.05**	**0.10**	**0.16**	**0.21**	**0.26**
C(2)-C(1)	-1.984	-1.986	-1.991	-2	-2.012	-2.026
C(3)-C(2)	-1.806	-1.805	-1.8	-1.792	-1.78	-1.767
C(3)-C(4)	-1.803	-1.802	-1.796	-1.788	-1.775	-1.76
C(4)-C(5)	-1.984	-1.986	-1.991	-1.998	-2.007	-2.018
C(1)-C(6)	-1.803	-1.801	-1.794	-1.785	-1.77	-1.754
C(5)-C(6)	-1.806	-1.803	-1.797	-1.787	-1.774	-1.759
C(6)-C(7)	-1.553	-1.552	-1.558	-1.572	-1.594	-1.62
C(7)-C(8)	-2.161	-2.161	-2.154	-2.141	-2.117	-2.089
C(8)-C(10)	-1.665	-1.663	-1.67	-1.685	-1.71	-1.74
C(10)-C(35)	-1.218	-1.219	-1.217	-1.217	-1.213	-1.211
C(10)-C(11)	-2.062	-2.069	-2.071	-2.064	-2.049	-2.025
C(11)-C(12)	-1.604	-1.593	-1.59	-1.599	-1.62	-1.653
C(13)-C(12)	-2.097	-2.107	-2.109	-2.105	-2.087	-2.063
C(35)-C(13)	-1.236	-1.236	-1.236	-1.235	-1.23	-1.227
C(9)-C(3)	-1.553	-1.562	-1.577	-1.599	-1.625	-1.653
C(16)-C(9)	-2.161	-2.154	-2.14	-2.12	-2.095	-2.067
C(17)-C(16)	-1.665	-1.673	-1.688	-1.708	-1.732	-1.756
C(38)-C(17)	-1.218	-1.217	-1.216	-1.213	-1.213	-1.21
C(18)-C(17)	-2.062	-2.05	-2.032	-2.011	-1.985	-1.957
C(19)-C(18)	-1.604	-1.619	-1.641	-1.667	-1.697	-1.727
C(19)-C(20)	-2.098	-2.083	-2.064	-2.04	-2.015	-1.987
C(20)-C(38)	-1.236	-1.236	-1.235	-1.231	-1.225	-1.219
C(13)-S(14)	-0.765	-0.753	-0.749	-0.749	-0.759	-0.778
S(21)-C(20)	-0.766	-0.783	-0.807	-0.838	-0.875	-1.389

Vol 11, Issue 5,May/ 2020
ISSN NO: 0377-9254

Au(15)-S(14)	-0.141	-0.145	-0.149	-0.15	-0.153	-0.154
S(21)-Au(22)	-0.141	-0.136	-0.13	-0.122	-0.112	-0.1

Wire 2 (W2)

Bonds	**0**	**0.05**	**0.10**	**0.16**	**0.21**	**0.26**
C(1)-C(2)	-1.983	-1.982	-1.986	-1.993	-2.004	-2.017
C(3)-C(2)	-1.812	-1.811	-1.807	-1.8	-1.79	-1.777
C(3)-C(4)	-1.81	-1.808	-1.803	-1.795	-1.785	-1.771
C(5)-C(4)	-1.982	-1.984	-1.988	-1.994	-2.003	-2.013
C(1)-C(6)	-1.809	-1.808	-1.803	-1.795	-1.784	-1.769
C(5)-C(6)	-1.812	-1.81	-1.805	-1.797	-1.787	-1.773
C(6)-C(7)	-1.543	-1.542	-1.545	-1.557	-1.575	-1.598
C(7)-C(8)	-2.189	-2.19	-2.188	-2.177	-2.161	-2.134
C(8)-C(10)	-1.645	-1.641	-1.643	-1.653	-1.671	-1.701
C(10)-S(14)	-0.675	-0.674	-0.676	-0.676	-0.675	-0.666
C(10)-C(11)	-1.985	-1.992	-1.995	-1.99	-1.979	-1.964
C(11)-C(12)	-1.769	-1.758	-1.756	-1.759	-1.769	-1.789
C(13)-C(12)	-2.011	-2.019	-2.022	-2.021	-2.012	-1.992
S(14)-C(13)	-0.649	-0.652	-0.654	-0.656	-0.658	-0.664
C(9)-C(3)	-1.543	-1.551	-1.565	-1.584	-1.607	-1.633
C(17)-C(9)	-2.188	-2.181	-2.168	-2.152	-2.13	-2.105
C(18)-C(17)	-1.644	-1.653	-1.666	-1.683	-1.704	-1.726
S(22)-C(18)	-0.675	-0.673	-0.67	-0.668	-0.664	-0.659
C(19)-C(18)	-1.985	-1.976	-1.963	-1.947	-1.929	-1.909
C(20)-C(19)	-1.77	-1.78	-1.795	-1.812	-1.831	-1.851
C(21)-C(20)	-2.011	-2	-1.986	-1.968	-1.949	-1.927
C(21)-S(22)	-0.648	-0.645	-0.642	-0.637	-0.631	-0.625
C(13)-S(15)	-0.836	-0.815	-0.806	-0.802	-0.807	-0.827
S(23)-C(21)	-0.833	-0.862	-1.344	-1.351	-1.355	-1.355
Au(24)-S(23)	-0.142	-0.138	-0.133	-0.126	-0.118	-0.109
S(15)-Au(16)	-0.144	-0.146	-0.148	-0.149	-0.149	-0.149

Table 4: Variance and balance parameter of W1 and W2 for various applied electric fields

W1			
EF(VÅ^{-1})	σ^2(+)	σ^2(-)	Balance parameter
0	84306.8	32.4	0
0.05	78645	37.1	0
0.1	0	0	0.24
0.16	0	0	0.25
0.21	0	0	0.25
0.26	175.5	234.7	0.24
W2			
EF(VÅ^{-1})	σ^2(+)	σ^2(-)	Balance Parameter
0	123.5 x10^6	20.141	2x10^{-6}
0.05	0.252	0	0
0.1	0	0	0.2
0.16	0	0	0.23
0.21	0.176	0	0
0.26	123.5 x10^6	20.141	2x10^{-6}